Evaluation of a vertical axis hydrokinetic turbine for water channels

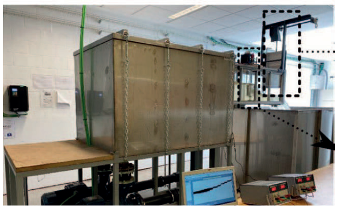

Evaluación de una turbina hidrocinética de eje vertical para su uso en canales

Aitor Fernández-Jiménez[1], Eduardo-Blanco-Marigorta[1], Ahmed Gharib Yosry[2], Víctor-Manuel Fernández-Pacheco[1] y Eduardo Álvarez-Álvarez[1]

[1] Universidad de Oviedo. GIFD. Departamento de Energía. Grupo de Ingeniería Fluido Dinámica. Área de Ingeniería Hidráulica. Calle Wifredo Ricart, s/n – 33203 Gijón (España).
[2] Universidad de Puerto Said. Dpto. Energía Mecánica. – 45526 Puerto Said (Egipto).

DOI: https://doi.org/10.6036/9635 Received: 30/07/2020 • Reviewing: 10/08/2020 • Acepted: 109/11/2020

To cite this article: To cite this article: FERNÁNDEZ-JIMÉNEZ, Aitor; BLANCO-MARIGORTA, Eduardo; GHARIB-YOSRY, Ahmed; FERNÁNDEZ-PACHECO, Víctor-Manuel; ÁLVAREZ-ÁLVAREZ, Eduardo. EVALUATION OF A VERTICAL AXIS HYDROKINETIC TURBINE FOR WATER CHANNELS. *DYNA*. March 2021, vol. 96 , no. 2, 6 pp. DOI: https://doi.org/10.6036/9883

RESUMEN

- El creciente interés por las energías hipocarbónicas ha sido fundamental para el desarrollo de nuevos sistemas de generación eléctrica a partir de fuentes renovables. En este contexto, las turbinas hidrocinéticas en canales son una excelente alternativa para poder suplir demandas en puntos aislados de la red. Estos sistemas, que aprovechan la energía de la corriente de agua, pueden ser instalados en canales hidráulicos, ríos o estuarios. El presente artículo realiza una caracterización experimental de una turbina hidrocinética en un túnel hidrodinámico en condiciones de baja velocidad de corriente, estimándose a su vez su comportamiento en el caso de un flujo sin restricciones. Los resultados muestran la gran importancia en la obtención de potencia del bloqueo de la corriente producida por la turbina
- Palabras Clave: turbinas hidrocinéticas, bloqueo, canales hidráulicos, baja velocidad.

ABSTRACT

The growing interest on low-carbon energy systems has been essential to develop new electricity devices based on renewable resources. In this context, channel turbines are an excellent alternative to supply demands that are isolated from power mains. These devices, which harness the kinetic term of the water current, can be installed in hydraulic channels, rivers, or estuaries.

This article carries out an experimental characterization of a hydrokinetic turbine in a hydrodynamic water tunnel under low velocity conditions, so its behavior under open field conditions can be obtained. The results show the relevance of the blockage effect made by the turbine during the power stage.
Key words: hydrokinetic turbines, blockage, water channels, low velocity

1. INTRODUCTION

1.1. ENERGIES FROM LOW-CARBON SOURCES. A BIG CHALLENGE

Faced with the prospect of global energy demand growth, especially in developing countries, the need arises to seek new alternatives to electricity production [1]. So far, only 21% of the world's energy is from renewable sources [2], but electricity from low-carbon technologies is expected to account for 40% of the world's total power generation park [3] by 2050. The growing interest in the development of green technologies has increased studies and developments focused on harnessing new sources for electricity generation without the use of fossil fuels. In addition, the tightening of environmental restrictions related to electricity generation has driven the research of new power generation systems.

Today, the most widely used renewable energy in the world is hydropower, representing 62% of all green electricity. However, it is expected that by 2050 this energy will only make up 28% of the renewable generation park [4]. This reduction meets economic and environmental criteria, as the construction of new reservoirs involves strong investments and significant impacts on ecosystems. That is why other technologies, such as solar or wind energy, will gain weight in all renewable energies as they require lower investments, maintenance and environmental impact.

If the projections made were met, the renewable energy sector could significantly increase its weight on Spain's Gross Domestic Product (GDP), a sector that currently generates about 18 billion euros per year. In addition, the development and implementation of these technologies could create more than 150,000 jobs (direct and indirect) and contribute to the reduction of CO2 emissions, meeting the objectives of the 2015 Paris Agreement [5]-[6]. It certainly seems that this sector will be key to continuing to fight the harmful effects of climate change.

1.2. HYDROKINETIC TURBINES IN CHANNELS. BET OF THE FUTURE

In this context there are other alternative low-carbon sources that, because of their enormous potential, could play a significant factor in the world's energy generation park. This is the case of energies from both marine and terrestrial water streams. For example, the European Ocean Energy Association (EOEA) estimates that, globally, up to 120,000 TWh could be generated from marine energies, being current energy the most important one [7].

To this marine potential should be added the water currents existing in terrestrial areas such as river, channels or water conductions (pipes), which could be used energetically.

For example, the National Renewable Energy Plan for 2011-2020 (PNER 2011-2020) has opted for the use of small low-power plants (< 1MW) in supply and sewer networks. In this way, it seeks to compatibilized the usual use of the installation with the generation of electricity, with a national potential of 840 MWh estimated in 2010 [8].

The most sustainable possibility of using water flowing currents under free sheet conditions, not requiring additional infrastructures to be built, are turbines that are designed to harness the kinetic term of the water current (speed) called hydrokinetic turbines [9]. The power obtained in these turbines will depend directly on the area swept by their blades, the speed of the water current, its density and the conversion efficiency of the equipment.

The U.S. Department of Energy defines a hydrokinetic turbine as a low-pressure turbine that harness the flowing current of a channel with low potential energy and a difference between upstream and downstream water heights less than 0.2 meters [10]. Finding current speeds high enough for be used is the main difficulty of these turbines, as they generally require speed values greater than 1.5 m/s [11]. On numerous occasions auxiliary mechanical or electrical elements, such as flow accelerators, must be installed in order to increase that speed so that the turbogenerator system can be installed [12].

Hydrokinetic turbines can be classified into two large types by comparing flow directions and axis of rotation: axial turbines (parallel flow and shaft) or cross-axis turbines (perpendicular flow and axis) (Figure 1).

Axial turbines have a design similar to horizontal axis wind turbines, available fully submerged, and being more efficient in energy conversion than cross-flow turbines. However, they require a complicated mechanical system for coupling the rotor with the generator, including both (system and generator) in a watertight capsule when submerged, which increases the cost these equipment and makes maintenance difficult [13].

Cross-flow turbines are based on rotor designs already known in the wind industry as vertical shaft turbines, for example, type: Savonius, Darrieus or Gorlov. In water, these turbines can be available with their shaft upright or horizontally. Although not as efficient as axial turbines, the simplicity of the mechanical rotor-generator coupling system reduces the cost of construction. In addition, vertical axis turbines located on farms allow greater use of the cross-sectional area of the current, being able to obtain power from currents with very low speed [14], and even a lower condition on the environment since their dimensions rarely exceed 2 meters in diameter [15].

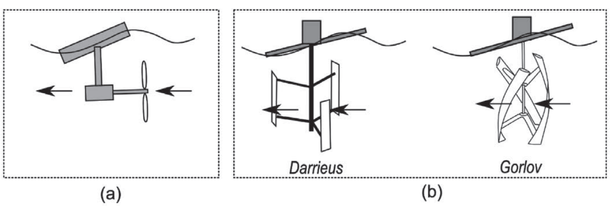

Fig. 1: Types of hydrokinetic turbine rotors (a) Axial and (b) Cross flow

Cross-flow turbines can be divided into two large typologies depending on the type of forces predominant in their blades for torque generation: drag or lift turbines [16]. On the one hand, drag turbines have as their main advantage their easy start-up rotation, while, on the other hand, lift turbines achieve higher yields. Examples of commercial designs include the Savonius rotor and Banki-Mitchell as drag turbines and the Darrieus and Gorlov rotor as lift turbines.

Another key aspect of lift turbines is the blade design, as aspects such as its geometry, solidity or angle of attack are key to the rotor's final performance [17].

On the one hand, there are numerous blade geometries that have been studied continuously both experimentally and numerically so that their aerodynamic behavior is known in the face of the incidence flow, such as the NACA (National Advisory Committee for Aeronautics , NACA) series [18]. On the other hand, the concept of solidity in turbines is a key factor in turbine performance [19]. Finally, studying the behavior of the blade angle variation as the turbine rotates is crucial for practicing geometry improvements and adjusting the position of the blades to the incidence of fluid [20].

This article shows the analysis and study of the performance of a Darrieus-type vertical axis cross-flow turbine in hydraulic channels, under blockage conditions and under low current speed conditions (< 1 m/s), which is very common in currents (channels, rivers). This type of turbines makes it significantly easier to extract energy from the hydrokinetic term of the water currents. The study has been carried out in a hydrodynamic tunnel installed in the laboratory of the Hydraulic Engineering Area of the Polytechnic School of Mieres (EPM, University of Oviedo).

2. THEORETICAL BASES

The tests have been carried out reproducing the flow conditions established in the one-dimensional model used in the demonstration of the actuator disc theory in a channel, proposed by the authors Houlsby, Draper and Oldfield [21] and representing the characteristics of the flow in the environment of a hydrokinetic turbine located in an area of a channel in which the flow was uniform and sub-critical prior to the installation of the equipment. This model considers (Figure 2):

- Disc submerged in water and blocked flow due to its presence.
- Two areas of uniform flow upstream and downstream of the turbine, as well as a flow mixing area once it has passed through the disc (located before the downstream).
- Subcritical flow and constant speed in the two uniform flow zones.
- The tests and characteristics of the testing channel allows to work in conditions very close to those indicated in the actuator disc theory:
- The different flow zones are obtained due to the performance on a gate located in the discharge of the channel.
- The low slope and its low roughness (built in glass) allow to assume a constant speed profile equal to the average speed in the sections of uniform flow upstream and downstream of the turbine.

The turbine characterization is performed from the ratio that relates the speed at the tip of the blade and the upstream flow speed ("Tip Speed Ratio"), the power coefficient and the mean and hydraulic mechanical powers of the current.

The following are the expressions for calculation.

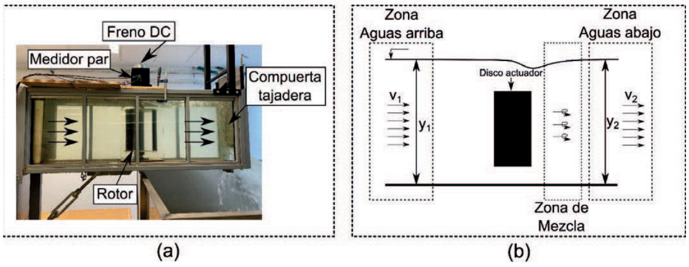

Fig. 2. Condition scheme for testing (a) hydrodynamic channel (b) actuator disc

$$TSR = \frac{\omega \cdot R}{v} \quad (1)$$

$$Cp = \frac{P_m}{P_t} \quad (2)$$

$$P_t = \frac{1}{2}\rho A_t v^3 \quad (3)$$

$$P\_m = \omega \cdot T \quad (4)$$

Where TSR is the speed ratio at the tip of the blade to the upstream (dimensionless) flow velocity, ω is the rotational speed of the rotor (rad/s), R is the radius of the turbine (m), v is the average current speed in the uniform upstream flow zone of the turbine (m/s), C_p is the power coefficient (dimensionless), P_m is the average mechanical power in a complete turbine turn (360º) (W), P_t is the hydraulic power of the current (W), ρ is fluid density (kg/m3), A_t is the area swept by blades (m2) and T is the torque at the axis (Nm). Note that the power in a cycle varies depending on the position of the turbine blades [22].

The dimensional parameters taken into account in the tests carried out are: current blockage, Reynolds number, Froude number, submerge coefficient and solidity; whose expressions are as follows:

and the user's clothing can cover the electronic module. The approximate cost of this laboratory prototype is only 200 €.

This device is the third version of wearable electronic tactile-foot interfaces that our team has implemented. This last version incorporates the technological improvements of the two previous developments [23, 24].

$$B = \frac{A_t}{A_c} = \frac{2R \cdot h}{b \cdot y} \quad (5)$$

$$Re = \frac{v \cdot c}{\mu} \quad (6)$$

$$F_r = \frac{v}{\sqrt{gy}} \quad (7)$$

$$C_h = \frac{y}{h} \quad (8)$$

$$\sigma = \frac{N \cdot c}{2\pi R} \quad (9)$$

Where B is the blockage coefficient (dimensionless), A_c is the full cross-section of the channel (m2), h is the rotor height (m), b is the width of the channel (m), y is the height of the water sheet in the uniform upstream flow zone (m), Re is Reynolds' number (dimensionless), c is the blade chord (m), μ is the kinematic viscosity of water (m2/s), F_r is Froude's number (dimensionless), g is the acceleration of gravity (m/s2), C_h is the coefficient of submergence (dimensionless), σ is solidity (dimensionless) and N is the number of blades in the turbine.

Once the tests have been carried out, the results obtained to estimate the operating characteristics of the turbine under open field conditions (without blockage) have been taken into account. Open field conditions are representative of large estuaries, where the flow is not restricted by the existence of walls or banks. However, under blockage conditions the fluid is constrained, so accelerations will appear around the turbine by forcing the flow to pass through the rotor [23]. This case is significant in low-width rivers and hydraulic channels.

For the aforementioned characterization under open-field conditions, C_p depending on TSR under that behavior can be obtained by using the following expressions:

$$Cp_F = C_p \left(\frac{v}{U}\right)^3 \quad (10)$$

$$TSR_F = TSR\left(\frac{v}{U}\right) \quad (11)$$

$$\frac{v}{U} = 1 - B \quad (12)$$

Where Cp_F is the power coefficient in open field (dimensionless), TSR_F is the speed ratio at the tip of the blade with the open-field's speed (dimensionless) and U is the open field velocity corresponding to operating conditions similar to those obtained with the blocked speed and for each value of the speed tested in the channel (m/s).

There are various relationships to estimate the equivalent speed in open field and blocked field conditions, using in this study the formulation proposed by Werle [24] (12) (one of the most used).

3. MATERIALS AND METHODS

3.1. TURBINE DESCRIPTION

The turbine studied has a rotor height and radius of h=0,3 m and R=0,15 m respectively, with N=3 blades (spaced 120 degrees) with a standard profile NACA 0015 and c=0,1 m chord, so its solidity is =0,318.

The selection of this profile meets simplification criteria of design and manufacture of the different parts that make up the rotor. The latest researches on water turbines indicates that, on the one hand, NACA 0015 profiles have better yields than asymmetric profiles under locking conditions [25] and, on the other hand, the use of three blades is much more advantageous in terms of efficiency and cost [26].

The turbine has been designed and printed using 3D technology based on nylon filament (PA). This material has been selected for its excellent durability in wet environments and its high resistance to continuous dynamic stresses. Due to 3D printing, different designs can be obtained quickly and cheaply to be experimentally tested, allowing research at a lower cost.

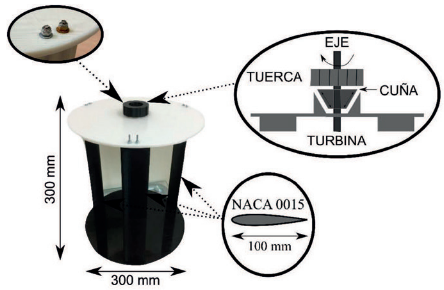

Fig. 3. Geometric characteristics of the turbine

The rotor couples to a 10 mm diameter metal axis of rotation using a wedge and nut system. This system, which has also been obtained by high precision 3D printing, allows the rapid exchange of different turbine designs, allowing to easily characterize different rotor designs. In addition, threaded rods have been used to ensure rotor integrity for joining the blades with the lower and upper turbine

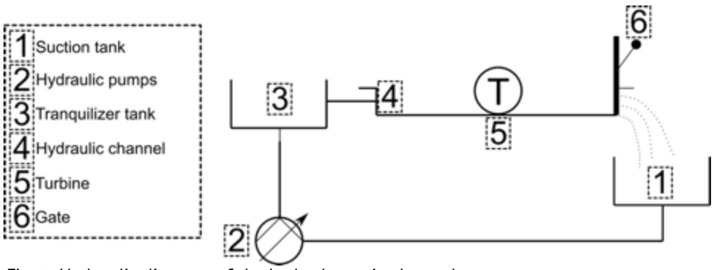

Fig. 4: Hydraulic diagram of the hydrodynamic channel.

The rotor couples to a 10 mm diameter metal axis of rotation using a wedge and nut system. This system, which has also been obtained by high precision 3D printing, allows the rapid exchange of different turbine designs, allowing to easily characterize different rotor designs. In addition, threaded rods have been used to ensure rotor integrity for joining the blades with the lower and upper turbine caps (see Fig 3).

3.2. DESCRIPTION OF THE HYDRODYNAMIC TUNNEL

The turbine has been characterized in a hydrodynamic tunnel located in the EPM (University of Oviedo). Its design meets low cost criteria, low current speed (< 1 m/s) and allows the testing of small vertical shaft rotors. It is similar to other tunnels such as the Canadian Hydrokinetic Turbine Test Centre (CHTTC) [27] and the one installed at the Missouri University of Science and Technology [28], all of them small in size and low current speeds.

The tunnel includes a rectangular section channel of 1.5 m length, 0.3 m wide and 0.55 m height. The walls and floor are made of laminated glass so that recording the different tests is allowed. Figure 4 shows a diagram of the tunnel hydraulic circuit.

The flow inside the channel is generated by a pumping equipment of 30 kW of total power, who is capable to move up 600 m3/h of water due to the installation of two hydraulic pumps (Pedrollo 120C series). Bombs suck water out of a 5 m3 suction tank and propel the fluid higher into a tranquilizer tank, from which water enters the channel freely falling back into the suction tank. It should be noted that the flow rate is regulated using electronic inverters (OMRON 3G3Rx series), being able to control the operation of the pumping equipment by varying the power supply frequency.

The turbines are anchored to the channel by using a low water resistance methacrylate box. This element has at its base a radial bearing specifically designed to work submerged that allows the turbine shaft to rotate in optimal conditions. Above, a lid is available where electronic measurement equipment and electric brake are installed. This system allows the quick and easy exchange of the rotors being completely detachable. Finally, at the free discharge point of the channel, a metal gate has been arranged, so the opening is controlled by a gear system to precisely control the discharge. This element is key to inducing low-speed hydrokinetic conditions (see Figure 5).

Fig. 5: Fig. 5. Descriptive photographs of the hydrodynamic tunnel.

3.3. CHARACTERIZATION METHOD USED

The turbine characterization process begins with an initial measurement, called "no-load" where no turbine-resistant torque is applied, obtaining the maximum value of TSR. Subsequently, and using the external DC power supply, the intensity value consumed by the brake is increased so that the brake's torque is increased successively. Thus, for each induced intensity you get a value of TSR and P_m. The process continues until the rotor stops completely, at which point the characterization test ends (see Figure 6).

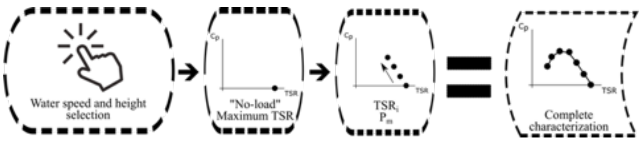

Fig. 6: Flowchart of the characterization of the power stage

A high-precision torque meter (MAGTROL TS 103 series) with a rated torque of 0.5 Nm and maximum torque of 1 Nm has been used for data collection. This instrument is calibrated by MAGTROL according to the standards of the Swiss Federal Institute of Metrology (METAS). This system measures resistant torque using a gauge by converting that value into an electrical signal whose electronic value is recorded. In addition, it features a high-frequency tachometer so that the turbine rotation speed and the relative position of the blades are instantly known during each full turn. This measurement is especially interesting for analyzing torque variation based on the situation of the blades during rotor rotation. A data-taking frequency of 80 data per second has been selected to obtain the spectrum of measurements as accurately as possible. The electric brake used and installed on the torque meter is the MAGTROL HB140M series.

4. RESULTS

The selected turbine has been characterized following the characterization procedure described above, in two tests with different speeds and keeping the position of the water sheet constant in the upstream area of the turbine and, therefore, the blockage produced by the turbine. It has not been possible to increase the number of tests due to the specific test conditions and characteristics of the hydrodynamic channel. Specifically:

Test 1: v=0,33 m/s, y=0,5 m, B=0,6, Re=3,2·10^4, F_r=0,14, C_h=1,66.

Test 2: v=0,40 m/s, y=0,5 m, B=0,6, Re=3,9· 10^4, F_r=0,18, C_h=1,66.

In the future, smaller rotors will be tested, but power measurement problems may occur as it will be significantly reduced and may not be accurately detected. Figure 7 shows the graphs P_m vs n (a), C_p vs TSR (b) and tables with some of the data calculated (c).

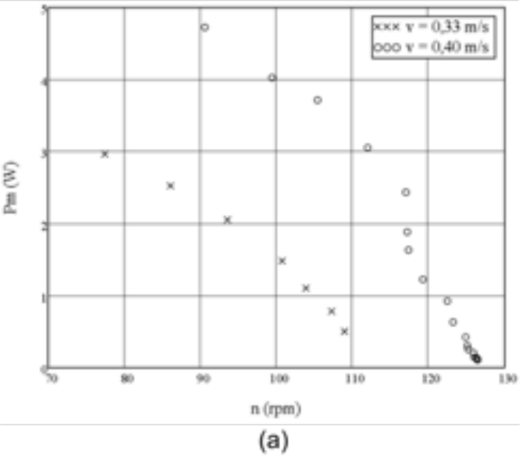

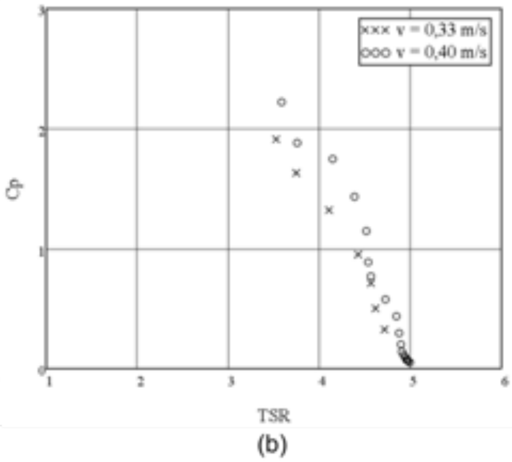

v = 0,33 m/s							
Nº test	T [N.m]	n [RPM]	Pm [W]	v [m/s]	TSR	Pt [W]	Cp
0	0,045	108,956	0,505	0,333	4,718	1,551	0,326
1	0,069	107,260	0,780	0,333	4,722	1,551	0,503
2	0,102	103,887	1,105	0,333	4,574	1,551	0,713
3	0,141	100,735	1,482	0,333	4,435	1,551	0,956
4	0,209	93,567	2,049	0,333	4,119	1,551	1,321

v = 0,4 m/s							
Nº test	T [N.m]	n [RPM]	Pm [W]	v [m/s]	TSR	Pt [W]	Cp
Vacio	0,008	126,440	0,103	0,370	5,010	2,127	0,048
1	0,009	126,410	0,121	0,370	5,009	2,127	0,057
2	0,010	126,301	0,139	0,370	4,989	2,127	0,065
3	0,011	126,025	0,143	0,370	4,994	2,127	0,067
4	0,016	126,261	0,208	0,370	5,003	2,127	0,098

(c)

Fig. 7: Graphs n vs Pm and Cp vs TSR for both speeds (a) and (b) and tables with calculated data (c)

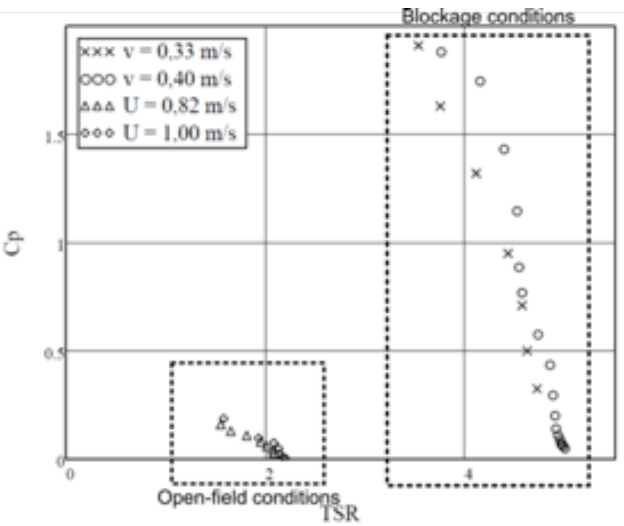

U = 0,82 m/s		
Nº test	TsrF	CpF
0	2,08	0,027
1	2,07	0,042
2	2,01	0,060
3	1,95	0,081
4	1,81	0,110
5	1,65	0,130
6	1,55	0,160

U = 1 m/s		
Nº test	TsrF	CpF
0	2,2	0,006
1	2,17	0,009
2	2,14	0,013
3	2,13	0,028
4	2,08	0,081
5	1,93	0,170
6	1,58	0,200

Fig. 8: Graph Cp vs TSR applying the Werle correction and tables with the calculated data

It can be seen how the turbine is able to generate maximum power values of 3 and 4 W under low water speed conditions (< 1 m/s), with high efficiency values (C_p=1,90 And C_p=2,21) that exceed the theoretical limit set by Betz de C_p=0,59. These circumstances show us the great importance of blockage conditions when energy is obtained from water streams.

The rotor is stopped in the tests carried out practically at the time when the maximum power produced is reached. This is due to the small value of its moment of inertia (reduced size and weight) in such a way that when the turbine starts working in the loss zone, the drag forces on the blades become very unstable and ends up slowing down [29].

Figure 8 shows the correction of the evolution of the power coefficient at open field conditions by applying the correction of the above-mentioned expression with the tables showing the calculated data.

It is noted that, after applying the mathematical corrections of the values of the power coefficient, these are considerably reduced obtaining practically a single curve that does not depend on the speed of the water (as it should correspond to an unrestricted open field) with a maximum Cp_F approximately 0.16 and 0.20 for open field speeds of 0.82 and 1.00 m/s respectively. These results are consistent with those obtained by Patel et al (2017) [25], where they used a rotor of geometry similar to the turbine presented (Darrieus with three blades of NACA 0015), obtaining a maximum power coefficient of 0.16 for a current speed of 0.46 m/s. In addition, TSR values higher the unit have been reached, so that, together with the existence of a stabled working area for higher TSR values, shows that in open field conditions the rotation would be generated by lift forces on its blades [30].

5. CONCLUSIONS

The development of hydrokinetic turbine-based systems for channels will allow the use of a large number of sites to cover demands at isolated points.

A three-blade turbine and NACA 0015 profile manufactured by additive 3D printing in a hydrodynamic tunnel under low-speed conditions (< 1 m/s) has been experimentally studied. Its characterization has been carried out by using of a high precision torque meter and a DC brake, testing two different water speeds, obtaining speed ratio values at the tip of the blade, power coefficient and medium and hydraulic mechanical powers.

The results shows the importance of current blockage conditions that allows to obtain power (up to 4 W) even in low speed conditions, with efficiencies that exceed the Betz limit.

In addition, the work has been completed by obtaining, from the data measured in the channel and through analytical relationships, the evolution of the power coefficient versus the TSR value to characterize the operation of the turbine model in open field without blocking effect.

Future researches seeks to adjust with the tests performed, a numerical model using computational fluid dynamics (CFD) techniques to analyze the fields of speeds and pressures in the turbine environment and perform different parametric studies that allow to vary characteristics of it (radio, height, rope of its blades) and flow conditions (height of the water sheet and speed). In addition, tests will be carried out with new rotor designs with the aim of improving the efficiency values obtained. Finally, the manufacture of a prototype of the system described for proof of concept at actual site is not ruled out.

References

[1] Organización de las Naciones Unidas. 2015. "Agenda de Desarrollo Sostenible". Ver: http://undocs.org/es/A/70/1 [Acceso 28 de Julio de 2020]

[2] International Energy Agency (IEA). 2019. "International Energy Outlook 2019".

[3] Muñiz, M. 2012. "Tres siglos de oro negro en piedra. El carbón en la oferta energética: pasado, presente y futuro". Facultad de Economía y Empresa. Universidad de Oviedo.

[4] Muñoz, L., Larracoechea, N. "Revisión y análisis de los sistemas de almacenamiento de energía mediante bombeo para soportar un mix de generación de electricidad con un alto porcentaje de energías renovables". 2019. DYNA, 94(6), 669-675. DOI: https://doi.org/10.6036/9182

[5] Alós, R. "El empleo en España en un horizonte 2025". 2019. Economía digital y políticas de empleo.

[6] MITECO. "Inventario Nacional de Gases de Efecto Invernadero. 2020. GEI"

[7] Caballero, C. "Estudio de plantas de producción de energías renovables con aprovechamiento de la energía del mar". 2011. Departamento de Electricidad. Universidad Carlos III, Madrid.

[8] Instituto para la Diversificación y Ahorro de la Energía (IDAE). Plan Nacional de Energías Renovables 2011-2020. 2011. Ver: https://www.idae.es/tecnologias/energias-renovables/plan-de-energias-renovables-2011-2020#:~:text=Renovables%202011%2D2020-,Plan%20de%20Energ%C3%ADas%20Renovables%20 2011%2D2020,aprovechamiento%20de%20las%20fuentes%20renovables [Acceso 28 de Julio de 2020].

[9] Mohammadi, S., Hassanalian, M., Arionfard, H. "Optimal design of hydrokinetic turbine for low-speed water Flow in Golden Gate strait". 2020. Renewable Energy, Vol 150, pp 147-155.

[10] Khan, M. J., Bhuyan, G., Iqbal, M. T., & Quaicoe, J. E. "Hydrokinetic energy conversion systems and assessment of horizontal and vertical axis turbines for river and tidal applications: A technology status review". 2009. Applied energy, 86(10), 1823-1835.

[11] Guney, M., Kaygusuz, K. "Hydrokinetic energy conversion systems: a technology status review". 2010. Renewable and Sustainable Energy Reviews, Vol 14, pp 2996-3004.

[12] Elbatran, A., Ahmed, M., Ahmed, S. 2017. "Performance study of ducted nozzle. Savonius water turbine, comparison with conventional Savonius turbine". 2017. Energy. Vol 134, pp 566-584.

[13] Lee, JH., Park, S., Kim, D., Dong, H. "Computational methods for performance analysis of horizontal axis tidal stream turbines". 2012. Applied Energy. Vol 98, pp 512-523.

[14] Balduzzi, F., Zini, M., Carbo, A. "Understanding the aerodynamic behavior and energy conversion capability of small Darrieus vertical axis wind turbines in turbulent flows". 2020. Energies. Vol 13, n 11.

[15] Sinagra, M., Sammartano, V., Arico, C., Collura, A., Tucciarelli, T. "Cross-flow turbine design for variable operating conditions". 2014. Procedia Engineering, 70, 1539-1548.

[16] Meana, A. "Optimized design of aerodynamic airfoils for vertical axis wind turbines". 2019. Universidad de Oviedo.

[17] Arpino, F., Scungio, M., Cortellessa, G. "Numerical performance assessment of an innovative Darrieus-style vertical axis wind turbine with auxiliary straight blades". Energy Conversion and Management. Vol 171, pp 769-777.

[18] Esteban, S. "Introducción a los perfiles NACA" 2011. Ingeniería Aeroespacial. Universidad de Sevilla.

[19] RC Marco, DB Stefano, B Ernesto. "Effect of Blade number on a straight-bladed vertical axis Darrieus turbine". 2012. World Academy of Sciences of Engineering Technologies. 61, 305 – 311.

[20] Battisti, L., Zanne, L., Castelli, M. "A generalized method to extend airfoil polars over the full range of angles of attack". 2020. Renewable Energy. Vol 155, pp 862-875.

[21] Houlsby, GT., Draper, S., Oldfield, MLG. "Application of linear momentum actuator disk theory to open channel flow". 2008. University of Oxford.

[22] Coiro, D., Nicolosi, F., De Marco, A., Melone, S., Montella, F. "Flow curvature effect on dynamic behaviour of a novel vertical axis tidal current turbine: numerical and experimental analysis". 2005. International Conference on Offshore Mechanics and Artic Engineering. Vol 41960, pp 601-609.

[23] Gauvin, O., Dumas, G. "Two-way interaction between river and deployed cross-flow hydrokinetic turbines". 2020. Journal of renewable and sustainable energy. Vol 12, n 3.

[24] Werle, MJ. "Wind turbine wall-blockage performance corrections". 2010. J Propuls Power. https://doi.org/10.2514/1.44602

[25] Patel V, Eldho, T, Prabhu, S. "Experimental investigations on Darrieus straight Blade turbine for tidal current application and parametric optimization for hydro farm arrangement". 2017. Int J Mar Energy. https://doi.org/10.1016/j.ijome.2017.01.007

[26] Burton, T., Sharpe, D., Jenkins, N y Bossanyi, E. "Wind energy handbook". 2001. Vol 2. New York: Wiley.

[27] Ver: http://www.chttc.ca/equipment.html [Acceso 2 de Noviembre de 2020].

[28] Hailong, Z. "Maximum power point tracking control of hydrokinetic turbine and low-speed high-trust permanent magnet generator design". 2016. Master of Science in Electrical Engineering. Missouri University of Science and Technology.

[29] Álvarez, E., Rico, M., Fernández, A., Espina, R., Corominas, E., Calleja, A. "Hydrodynamic water tunnel for characterization of hydrokinetic microturbines designs". 2020. Clean Technologies and Environmental Policy. https://doi.org/10.1007/s10098-020-01924-w

[30] Kumar, A., Saini RP. "Performance parameters of Savonius type hydrokinetic turbine – A review". 2016. Renewable and Sustainable Energy Reviews, 64, 289-310.

[22] Kennedy P.M., Inglis J.T., "Distribution and behaviour of glabrous cutaneous receptors in the human foot sole". Journal of Physiology. February 2002, Vol. 538-3, p. 995-1002. DOI: https://doi.org/10.1113/jphysiol.2001.013087

[23] Velazquez R, Bazan O, Varona J, et al. "Insights into the capabilities of tactile-foot perception". International Journal of Advanced Robotic Systems. August 2012, Vol. 9, p. 1-11. DOI: https://doi.org/10.5772/52653

[24] Velazquez R, Pissaloux E, Lay-Ekuakille A. "Tactile-foot stimulation can assist the navigation of people with visual impairment". Applied Bionics and Biomechanics, February 2015, Vol. 2015, p. 1-9. DOI: http://dx.doi.org/10.1155/2015/798748